Desalination and Water Treatment
www.deswater.com

doi: 10.5004/dwt.2017.20270

65 (2017) 259–266
February

Removal of iron and manganese from aqueous solution using some clay minerals collected from Saudi Arabia

Mohamed A. Embaby[a,b], Hany H. Abdel Ghafar[a,c], Mohamed M.E. Shakdofa[a,d], Nagy M. Khalil[a,e], Emad K. Radwan[c,*]

[a]*Department of Chemistry, Faculty of Sciences and Arts, Khulais, University of Jeddah, Saudi Arabia, emails: embaby_mn@yahoo.com (M.A. Embaby), hany_ghafar@hotmail.com (H.H.A. Ghafar), mshakdofa@yahoo.com (M.M.E. Shakdofa), nagy2071@yahoo.com (N.M. Khalil)*
[b]*Department of Food Toxicology and Contaminants, National Research Centre, 33 El Bohouth St, Dokki, Giza, Egypt 12622*
[c]*Department of Water Pollution Research, National Research Centre, 33 El Bohouth St, Dokki, Giza, Egypt 12622, Tel. +202 33370931; Fax: +202 33371211; email: emadk80@gmail.com*
[d]*Department of Inorganic Chemistry, National Research Centre, 33 El Bohouth St, Dokki, Giza, Egypt 12622*
[e]*Department of Refractories, Ceramics and Building Materials, National Research Centre, 33 El Bohouth St, Dokki, Giza, Egypt 12622*

Received 13 May 2016; Accepted 16 October 2016

ABSTRACT

The existence of excessive concentrations of iron and manganese in water results in economic, technological and health problems. The adsorption characteristics of four clay minerals collected from different localities of Saudi Arabia, Osfan (OS1 and OS2) and Gholaa (GH1 and GH2), on the adsorption of Fe^{3+} and Mn^{7+} ions were investigated. The quantitative phase composition of the selected samples was calculated from their X-ray diffraction technique, while the chemical constitution was determined through X-ray fluorescence technique. The adsorption of Fe^{3+} onto different clays was complied with Langmuir isotherm (R^2 = 0.9996, 0.9956, 0.9840 and 0.9932, respectively). OS1 and OS2 (Q_{max} = 6.872 and 8.258; 1/*b* = 0.315 and 0.296, respectively) have higher adsorption capacity than GH1 and GH2 (Q_{max} = 2.109 and 3.457; 1/*b* = 0.596 and 0.465, respectively). The adsorption of Fe^{3+} onto OS1, OS2, GH1 and GH2 clay minerals cannot be described by Freundlich isotherm model where R^2 = 0.831, 0.92, 0.70 and 0.52, respectively. The mean adsorption energy recorded indicates that the sorption process is physisorption.

Keywords: Natural minerals; Adsorption; Heavy metals; Freundlich; Langmuir; Sorption capacity; Water treatment

1. Introduction

The occurrence of iron and manganese in natural water can be attributed to the weathering of rocks and minerals where the iron and manganese dissolved by the water passing through soil and rock enter groundwater supplies [1,2]. Moreover, iron and manganese are present in drinking water due to anthropogenic sources, including acid mine drainage [3] landfill leachates [4], industrial and sewage effluents [5], and as a consequence of the corrosion of the metal pipes used for transferring the drinking water [6].

The World Health Organization (WHO) and the Environmental Protection Agency (EPA) have set a standard levels of 0.3 and 0.05 mg/L of iron and manganese, respectively [7,8]. On the other hand, the European Union has recommended the levels of 0.2 and 0.05 mg/L for iron and manganese, respectively [9]. The existence of excessive concentrations of iron and manganese in water results in economic, technological and health problems.

The technological problems include failure of water supply systems process and water quality decline. For example, in the presence of somewhat high concentrations of oxygen, they form undesirable dark sludge, which impacts the growth of ferruginous and manganese bacteria on the walls of the pipes [10].

* Corresponding author.

These bacteria change the water quality (smell), enhance the corrosion of the pipes and gradually reduce the flow rate through the pipes [11]. In addition, the excessive concentrations of iron and manganese will result in metallic taste in water and can cause staining of laundry, utensils, dishes, paper, plastics and glassware [12,13]. Moreover, the color and flavor of food and water can be affected by iron and manganese, because they can react with tannins in coffee, tea and alcoholic beverages.

Health effects resulting from the chronic exposure to high manganese include toxicity to the nervous system [14], lethargy, increased muscle tonus, tremor, mental disturbances [15] and difficulties in both visual and verbal memory [16].

Iron and manganese often ordinarily exist in groundwater. Consequently, the iron and manganese treatment techniques are closely connected [17]. Conventional techniques of iron and manganese removal include chemical precipitation, ion exchange, crystallization and electrochemical process [18]. These techniques are based on the transformation of iron and manganese into undissolved compounds. Then, the undissolved compounds can be removed by one- or two-stage separation [19]. Numerous treatment processes, such as ozonation [20,21] and electric discharge [22,23], have been employed for groundwater treatment. Yet, the costs of energy consumption and operation and maintenance of the apparatus limit the use of these processes. Natural minerals are considered as perspective sorbents for different impurities removal due to their widespread, cheapness and high sorption properties. On the other hand, granular activated carbon is often used to enhance the removal of Mn^{2+} from water [24–26]. However, the drawback is frequent regeneration or new carbon replacement. The ion exchange characteristics of clays have been extensively investigated [27]. Exchange type, operating conditions and the metal being removed affect the ion exchanger degree of preference for each metal ion [28].

In the current study, the ability of some clay minerals from different localities of Saudi Arabia to eliminate iron and manganese from aqueous solution has been investigated in a batch process. Furthermore, the effect of contact time, initial metal concentration and clay dosage on the adsorption characteristics have been assessed. The adsorption isotherm and thermodynamic parameters were deduced from adsorption measurements.

2. Materials and methods

2.1. Raw materials (clay minerals)

Four raw material batches were taken from different regions in Khulais Governorate, Saudi Arabia. Two batches were taken from near Osfan and designated as OS1 and OS2, and two batches were taken from Gholaa and designated as GH1 and GH2.

2.2. Chemicals

All chemicals used throughout the experimental works were of analytical grade provided by Merck (Darmstadt, Germany). Iron and manganese salt used in the preparation of the synthetic metal bearing stock solution (1,000 mg/L) were $Fe(SO_4)_2NH_4{\cdot}12H_2O$ and $KMnO_4$. The working solutions were prepared by diluting the stock solutions. Deionized water was used throughout the experimental work. Standard solutions of Fe^{3+} and Mn^{7+} (1,000 mg/L) for atomic absorption spectrophotometer were obtained from Merck, Germany.

2.3. Processing of the raw materials

The individual rocks were manually crushed to reach grain size of approximately 5–10 mm in diameter. The crushed briquettes were ground in a high-speed, shimmy sintered alumina ball mill (MTI Corporation, USA) with sintered alumina balls as grinding medium. The grinded samples were sieved through a 75-micron standard sieve; the residues were returned to the ball mill for further milling until the sample completely passed through the sieve. Representative samples of 50 g of each sample, through quartering process, were taken to represent the mother batch.

2.4. Investigation of the raw samples

The representative samples of the processed raw materials were investigated for their mineralogical compositions using X-ray diffraction (XRD) technique (A Phillips PW 1710 diffractometer with Ni filtered Cu-KαX-radiation operating at 30 mA and 40 kV). Based on the phase composition results, four samples were selected for further investigation. Quantitative phase compositions were calculated from the XRD patterns. Chemical analysis was determined using Philips PW 1480 wavelength dispersive X-ray fluorescence (XRF) spectrometer. Scanning electron microscope (SEM; A Philips XL30 scanning electron microscope attached with energy-dispersive X-ray [EDX] unit with accelerating voltage 30 kV and magnification up to 20.000x) was used to study the morphology of one selected sample.

2.5. Batch adsorption studies

The batch adsorption studies were carried out at room temperature (25°C ± 0.1°C) by contacting the clay with metal ions in 250 mL stopper conical flasks. The samples were shook at 120 rpm using mechanical shaker and filtered, and the Fe^{3+} and Mn^{7+} concentration was measured in the filtrate. To differentiate between possible metal precipitation and actual metal sorption, control (blank) was used without clay materials. All the experiments were carried out in triplicate, and the mean of the quantitative results were reported and used for further calculations. Standard deviation of results was calculated, and if its value was greater than 5%, the data were neglected.

The concentration of Fe^{3+} and Mn^{7+} in all samples was determined according to the American Public Health Association (APHA) method [29] using atomic absorption spectrophotometer (Agilent SpectrAA 220, USA) with deuterium arc background corrector. The accuracy and precision of iron measurement were confirmed using National Institute of Standards and Technology (NIST) certified standard reference material (SRM) 1643e trace elements in water.

2.5.1. Effect of contact time

The effect of contact time was carried out by conducting batch adsorption experiments with Fe^{3+} and Mn^{7+} concentrations of 20 mg/L, 0.4 g/L clay and at different time intervals (10, 30, 50, 70, 90 and 120 min).

2.5.2. Effect of adsorbent dosage

The adsorbents dosage was varied from 0.05 to 0.5 g using a fixed volume of 100 mL of 20 mg/L of metal solution at equilibration time and natural pH (3.35 and 3.44 for Fe^{3+} and Mn^{7+}, respectively).

2.5.3. Adsorption isotherms

Isotherms were measured by varying the initial metal ion concentrations at the optimum conditions. Different adsorption models were used for comparison with experimental data such as Langmuir, Freundlich and Dubinin–Radushkevich (D–R) [30].

Langmuir isotherm relationship is given as:

$$C_e / C_{\text{ads}} = 1/Q_b + C_e / Q \quad (1)$$

where C_e (mg/L) is the concentration of metal in solution at equilibrium; C_{ads} (mg/g) is the amount of metal sorbed per unit mass of adsorbent; and Q (mg/g) and b are Langmuir constants related to mono layer capacity sorption and sorption energy, respectively.

Linear Freundlich isotherm relationship is given as:

$$\log q_e = \log K_f + 1/n \log C_e \quad (2)$$

where K_f and n are the Freundlich constants and are related to the adsorption capacity of the sorbent and the adsorption intensity.

The linearized D–R isotherm equation can be written as:

$$\ln q_e = \ln X_m - \beta\varepsilon^2 \quad (3)$$

where q_e is the amount of metal ions adsorbed per unit mass of adsorbent (mol/g); X_m is the maximum sorption capacity; β is the activity coefficient related to mean sorption energy; and ε is the Polanyi potential, which is:

$$\varepsilon = RT\ln(1+1/C_e) \quad (4)$$

where R is the gas constant (J/mol K), and T is the temperature (K). The saturation limit X_m may represent the total specific micro pore volume of the sorbent.

The sorption energy can also be calculated using the following equation:

$$E = \frac{1}{\sqrt{-2\beta}} \quad (5)$$

3. Results and discussions

3.1. Phase and chemical compositions

3.1.1. Quantitative phase composition

Table 1 shows the quantitative phase composition of the studied samples calculated from their XRD patterns. OS1 and OS2 are composed mainly of albite (56.0% and 63.5%, respectively) while GH2 contains the lowest proportion of albite (18.6%) among the four investigated samples. Kaolinite, quartz, albite and tremolite (in comparable proportions) are the main phases constitute GH2 sample. OS2 contains considerable comparable contents of chlorite (13.8%) and tremolite (13.6%) with relatively lower content of chamosite (9.1%). OS1 contains considerable content of chamosite (17.6%), little contents of quartz (6.3%) and biotite (4.2%) in addition to very little content of hematite (1.7%).

3.1.2. Chemical constitution

Table 2 displays the chemical constitution of the studied clays as determined by XRF technique.

The results show that the samples composed mainly of silica (SiO_2 ≈ 47%–56%) and alumina (Al_2O_3 ≈ 14%–17%). They also contain considerable amounts of iron oxide (Fe_2O_3 ≈ 10%–17%), sodium oxide (Na_2O ≈ 10%–17%), calcia (CaO ≈ 1%–5%), magnesium oxide (MgO ≈ 3%–8%), potassium oxide (K_2O ≈ 0.5%–1.5%) and titania (TiO_2 ≈ 1%–1.5%) in addition to little contents of other impurities that do not exceed together ≈2%. The loss on ignition ranges between 2.4% and 3.8%.

The results also indicate that GH2 contains the highest proportion of silica (56.653%) followed by OS1 (51.082%),

Table 1
Phase percentage of the studied clays

Phase	wt%			
	OS1	OS2	GH1	GH2
Albite ($NaAlSiO_3$)	56.0	63.5	85.4	18.6
Quartz (SiO_2)	6.3	–	–	22.2
Chlorite ($Mg_6Si_4O_{10}(OH)_8$)	14.2	13.8	8.8	11.6
Chamosite ($Fe_3Si_2O_5(OH)_4$)	17.6	9.1	–	–
Tremolite ($Na_{0.11}Ca_{1.69}Mg_{4.6}Fe_{0.48}Al_{0.29}Si_{7.82}O_{22}(OH)_2$)	–	13.6	5.8	17.8
Biotite ($H_4K_2Mg_6Al_2Si_6O_2$)	4.2	–	–	–
Hematite (Fe_2O_3)	1.7	–	–	–
Kaolinite ($Al_2Si_2O_5(OH)_4$)	–	–	–	23.8
Illite ($KAl_2Si_3AlO_{10}(OH)_2$)	–	–	–	5.1
Anatase (TiO_2)	–	–	–	0.8

Table 2
Chemical compositions of the studied clay samples

Constituents (wt%)	OS1	OS2	GH1	GH2
Na_2O	4.015	5.624	4.328	3.127
MgO	8.550	5.756	4.864	3.642
Al_2O_3	17.008	15.571	14.009	14.367
SiO_2	51.082	49.811	47.080	56.653
P_2O_5	0.456	0.317	0.379	0.320
SO_3	0.099	0.037	0.100	0.026
K_2O	1.879	0.493	0.540	1.288
CaO	1.400	3.757	4.183	5.991
TiO_2	1.394	1.207	1.454	0.974
Cr_2O_3	0.016	–	–	0.019
MnO	0.335	0.477	0.674	0.263
Fe_2O_3	10.406	13.577	17.813	10.120
Co_3O_4	0.024	0.030	0.033	0.033
NiO	–	–	–	0.020
CuO	0.013	0.016	0.029	0.019
ZnO	0.033	0.043	0.069	0.029
Rb_2O	–	–	–	0.004
SrO	0.023	0.018	0.028	0.095
ZrO_2	0.071	0.021	0.039	0.022
BaO	0.047	0.024	0.023	0.044
F	0.204	0.451	0.380	0.497
Cl	0.450	0.700	0.174	0.048
L.O.I	2.900	2.700	3.800	2.400

while samples OS2 and GH1 contain relatively lower proportions of silica (49.811% and 47.080%). On the other hand, OS1 sample contains the highest proportion of alumina (17.008%) followed by OS2 sample (15.571%) while GH1 and GH2 contain relatively lower proportions of alumina (14.009% and 14.367%). These results are in a good agreement with the quantitative phase compositions (see Table 1). All the samples contain different amounts of albite resulting from the combination between sodium oxide, aluminum oxide and silicon oxide. Albite is the main constituent of OS1, OS2 and GH1 while its content is relatively lower in GH2. The sample GH2 contains a relatively higher content of quartz (22%) and kaolinite (23%) (Table 1); this is confirmed by the highest percentage of silicon oxide content in this sample (56.653%, Table 2). The relatively higher contents of iron oxide in the four samples verify the presence of iron containing minerals, e.g., hematite, chamosite or tremolite. The presence of considerable quantities of magnesium oxide in the four samples is an indication of the presence of magnesium containing minerals namely chlorite, biotite and tremolite while the presence of calcium oxide and potassium oxide is related to the existence of tremolite and illite minerals, respectively.

3.2. Effect of adsorbent dosage

The percentage of removal of Mn^{7+} by the clays under study was very low, even at the highest dosage of the adsorbent (0.5 g/100 mL), where the highest removal percentage recorded was 35.4 at 120 min for OS2 (data not shown). The effect of the adsorbent dosage on the removal of Fe^{3+} is shown in Fig. 1.

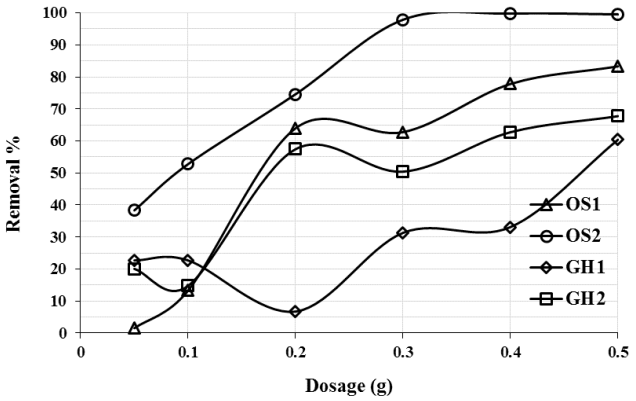

Fig. 1. Effect of clay dosage on the removal of Fe^{3+} from aqueous solution (C_0 = 20 mg/L, contact time 10 min for OS1 and OS2, 70 min for GH1 and GH2, at 24°C).

At lower clay dosage (0.05–0.3 g/100 mL) of OS1 and OS2, the curves have a relatively high slope, while at higher dosage the slope was relatively low with obvious plateau. In other words, at lower clay dosage, the removal percentage increases greatly with increasing the dosage. While at high dosage the removal percentage slightly increased.

The highest removal percentage recorded for OS1 GH1 and GH2 was 83.3, 60.4 and 67.75 at 0.5 g/100 mL, respectively. While the highest removal percentage recorded for the OS2 was 99.78 at 0.4 g/100 mL, yet, the recorded removal percentage for the OS2 at 0.3 g/100 mL was 97.87.

The adsorption of Fe^{3+} ions increased with increasing the clay dosage due to increasing the clay surface area available for binding to Fe^{3+} ions. While in case of Mn^{7+} ions, there is no significant change even by increasing the adsorbent amount up to 1.2 g/100 mL. The higher adsorption affinity of the clay minerals toward Fe^{3+} might be due to: (a) the bigger ionic radius of Fe^{3+} compared with Mn^{7+} and/or (b) the higher electronegativity of Fe^{3+} compared with Mn^{7+}. The bigger atomic radius of Fe^{3+} diminishes its hydration capacity, consequently, weakens the binding of Fe^{3+} and water phase, and strengthens the adsorption of Fe^{3+} on the clay. Similar pattern have been reported beforehand [31]. On the other hand, it has been reported that the adsorption affinity increases with increasing the electronegativity [32].

3.3. Effect of contact time

Fig. 2 displays the effect of contact time on the adsorption of Mn^{7+} by different mineral clays. The adsorption of Mn^{7+} on all mineral clays (OS1, OS2, GH1 and GH2) is weak where the maximum removal percentages recorded were 35.0, 35.4, 27.33 and 26.8, respectively. The maximum removal percentages were at 50 min for all clays except OS2 was at 120 min.

The effect of contact time on the adsorption of Fe^{3+} by different adsorbent clays is shown in Fig. 3. The adsorption of both OS1 and OS2 was rapid, and the equilibrium was reached at the first 10 min, where the removal percentage recorded 91 and 100, respectively. Whereas for GH1 and GH2,

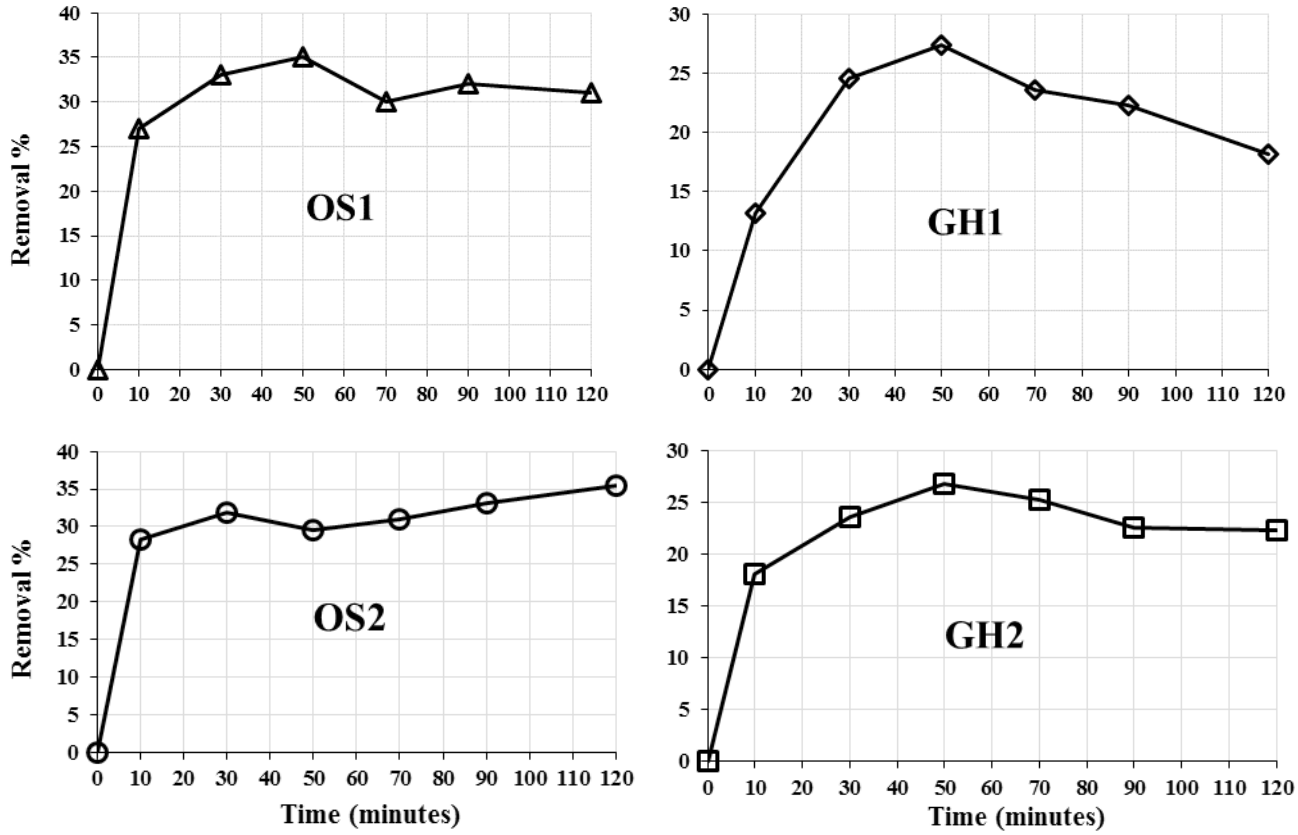

Fig. 2. Effect of contact time on Mn^{7+} removal by clay minerals (C_0 = 20 mg/L, 0.3 g clay, at 24°C).

the removal percentage was increased gradually from 37.8 and 36.7 at 10 min to 78.66 and 80.12 at 120 min, respectively.

The abovementioned results indicated that the clays OS1 and OS2 have a strong ability to bind Fe^{3+} in shorter time than GH1 and GH2, and can be used for removal of iron from water. The albite content was 56%, 63.5%, 85.4% and 18.6% for OS1, OS2, GH1 and GH2, respectively (Table 1). Sample GH1 with the highest content of albite 85% showed the lowest affinity toward Fe^{3+}. The strong ability of OS1 and OS2 to bind Fe^{3+} cannot be explained in terms of chemical composition because the four samples composed mainly of albite with small contents of different minerals. The high affinity of samples OS2 and OS1 toward Fe^{3+} might be related to the type and size of pores formed due to the dissolution of some impurities in aqueous solution during the treatment process.

3.4. Equilibrium studies and isotherm modeling

The adsorption isotherms were modeled by Langmuir, Freundlich and D–R equations. The Freundlich and Langmuir are the most commonly applied models to depict the relationship between equilibrium adsorption capacity (q_e, mg/g) and final concentrations (C_e, mg/L) at equilibrium [33]. The D–R model was applied to expect the nature of adsorption processes as physical or chemical [34]. The equilibrium studies and isotherm modeling in the current study focused on Fe^{3+} adsorption rather than Mn^{7+} because Fe^{3+} showed higher adsorption than Mn^{7+}.

3.4.1. Langmuir isotherm

Langmuir model suggests that sorption takes place homogenously on the active site of the adsorbent, and once an adsorbate occupies a site, no more adsorption occurs on this site [35]. The Langmuir parameters, b and Q_{max}, give information about the affinity and uptake capacity of the adsorbent. A high value of Q_{max} and b means that the adsorbent has high adsorption capacity and that the affinity between the adsorbent and adsorbate is high, respectively [36].

Fig. 4 and Table 3 show that the adsorption of Fe^{3+} onto different clays (OS1, OS2, GH1 and GH2) obeyed Langmuir isotherm (R^2 = 0.9996, 0.9956, 0.9840 and 0.9932, respectively). Also, the OS1 and OS2 (Q_{max} = 6.872 and 8.258, respectively) have higher adsorption capacity than GH1 and GH2 (Q_{max} = 2.109 and 3.457, respectively). Moreover, the affinity between the Fe^{3+} and the OS1 and OS2 ($1/b$ = 0.315 and 0.296, respectively) is higher than that of the GH1 and GH2 ($1/b$ = 0.596 and 0.465, respectively). These results proved that OS1 and OS2 are promising adsorbents for the removal of Fe^{3+} from aqueous solutions.

3.4.2. Freundlich isotherm

Likewise to Langmuir, the values of the Freundlich parameters (K_f and n) give information about the adsorption capacity and the affinity between the adsorbent and adsorbate [37]. A high value of K_f and n means that the adsorbent have high adsorption capacity and that the affinity between

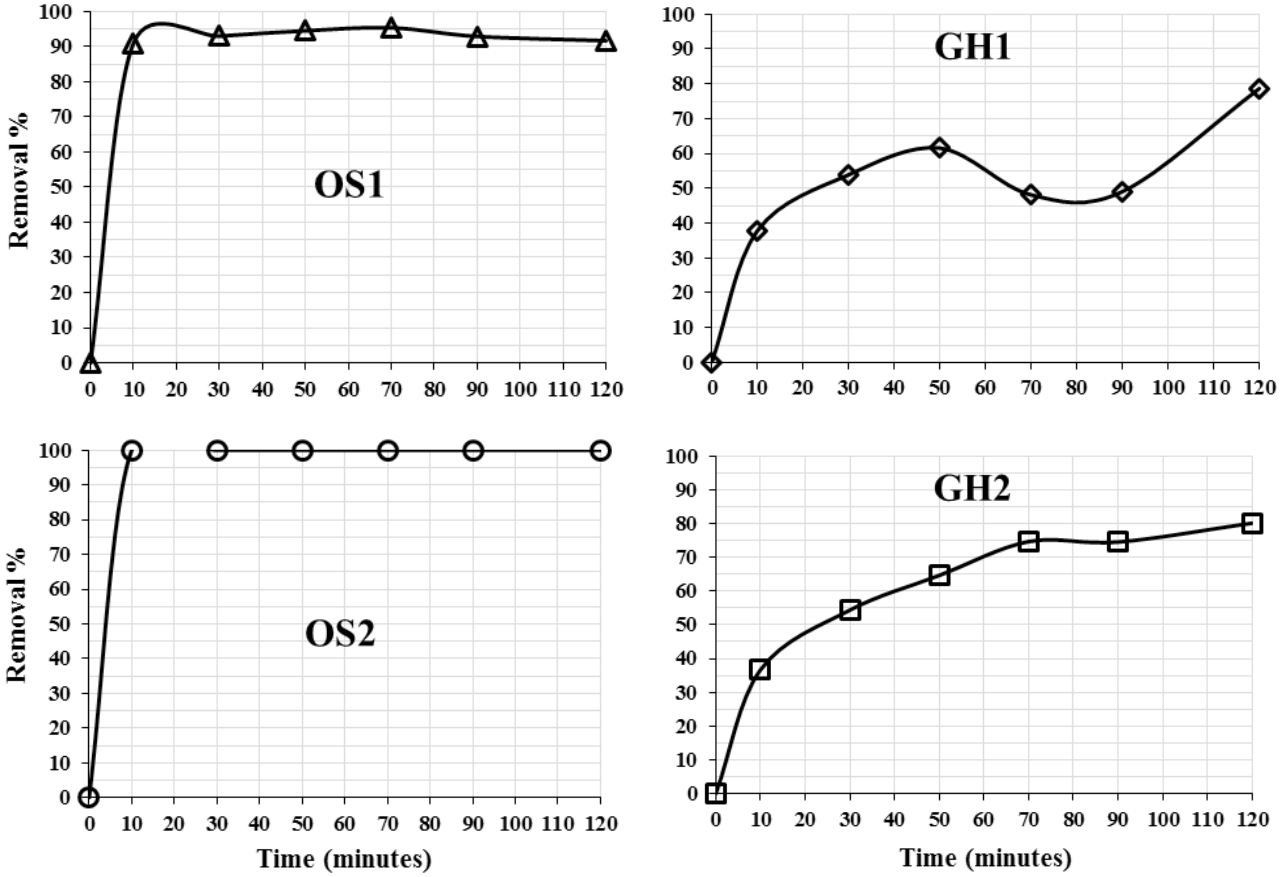

Fig. 3. Effect of contact time on Fe^{3+} removal by clay minerals (C_0 = 20 mg/L, 0.3 g clay, 24°C).

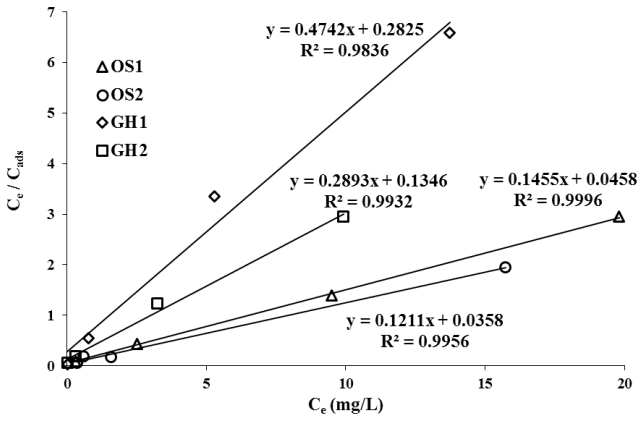

Fig. 4. Langmuir model for the adsorption of Fe^{3+} by clay minerals (clay dosage: 0.3 g/100 mL, contact time 120 min, at 24°C).

the adsorbent and adsorbate is high, respectively. According to Table 3, the R^2 (0.831, 0.92, 0.70 and 0.52) values indicated that Freundlich model cannot describe the adsorption of Fe^{3+} into clay minerals.

3.4.3. D–R isotherms

Unlike Freundlich and Langmuir models, the value of the D–R model parameter (mean free energy of adsorption [*E*]) gives information about the nature of adsorption processes as physical or chemical. The data illustrated in Table 4 represents the D–R plot of the adsorption of Fe^{3+} onto different clays. The positive values of *E* indicated that the adsorption of Fe^{3+} into the clay is endothermic and that higher solution temperature will favor the adsorption process [38]. The mean adsorption energy recorded was 17.9374, 20.6550, 17.0800 and 17.1340 kJ/mol for OS1, OS2, GH1 and GH2 clays, respectively (Table 4). The clay samples have adsorption energies <40 kJ/mol, which indicate that the sorption process is physisorption [39,40].

4. Conclusions

The current study investigated the ability of some minerals clays collected from Saudi Arabia to remove iron and manganese ions from aqueous solution. The results showed that the Fe^{3+} ions were more adsorbed than Mn^{7+} ions on the minerals clays under investigation (OS1, OS2, GH1 and GH2), and the maximum removal percentages recorded were 35.0, 35.4, 27.33 and 26.8, for Mn^{7+}, while for Fe^{3+} were 91, 100, 78.66 and 80.12, respectively.

The OS1 and OS2 have a higher affinity toward Fe^{3+} ions than GH1 and GH2. The adsorption data were perfectly described by Langmuir adsorption isotherm indicating a formation of monolayer adsorption of Fe^{3+} ions on clay samples. The maximum adsorption capacity was 6.872, 8.258, 2.109

Table 3
Summary of isotherm model parameters for clay minerals adsorbents

Clay	Freundlich model			Langmuir model		
	K_f	$1/n$	R^2	Q_{max} (mg/g)	$1/b$	R^2
GH1	1.4105	0.1258	0.8312	2.109	0.596	0.9840
GH2	1.9502	0.2029	0.9246	3.457	0.465	0.9932
OS1	5.7557	0.0503	0.7031	6.872	0.315	0.9996
OS2	7.1845	0.0345	0.5203	8.258	0.296	0.9956

Table 4
Summary of D–R model parameters for the removal of Fe^{3+}

Clay	X_m (mol/g)	β (mol^2/j^2)	Sorption energy (E, KJ/mol)
GH1	7.833×10^{-5}	-0.1713×10^{-8}	17.0800
GH2	7.1087×10^{-5}	-0.1703×10^{-8}	17.1340
OS1	2.391×10^{-4}	-0.1554×10^{-8}	17.9374
OS2	2.538×10^{-4}	-0.1172×10^{-8}	20.6550

and 3.457 mg/g for OS1, OS2, GH1 and GH2, respectively, as calculated from Langmuir isotherm model. The adsorption of Fe^{3+} to clay samples follows the order OS2 > OS1 > GH2 > GH1. The D–R model indicated that the adsorption takes place physically and the sorption energy was in the order OS2 > OS1 > GH2 > GH1 supporting the Langmuir isotherm model. A further deep study is in needed to explain this order and high affinity of Osfan samples toward Fe^{3+} ions.

Acknowledgments

This work was funded by King Abdulaziz City for Science and Technology (KAST), KSA, under grant No. 34–56. The authors, therefore, acknowledge with thanks KAST for technical and financial support.

Conflicts of interest

The authors declare that they have no conflict of interest.

References

[1] A. Kowal, M. Świderska-BróŜ, Water Purification, PWN, Warsaw and Wroclaw, 1996.
[2] L. Magrel, Water Treatment and Wastewater Treatment, Equipment, Processes, Methods, Economics and the Environment, Bialystok, 2000.
[3] M. Ahmad, Iron and Manganese Removal from Groundwater: Geochemical Modeling of the Vyredox Method, Master Thesis, Department of Geosciences, University of Oslo, 2012.
[4] S.C. James, Metals in municipal landfill leachate and their health effects, Am. J. Public Health, 67 (1977) 429–432.
[5] B. Oliver, E. Cosgrove, Metal concentrations in the sewage, effluents, and sludges of some southern Ontario wastewater treatment plants, Environ. Lett., 9 (1975) 75–90.
[6] M. Lasheen, C. Sharaby, N. El-Kholy, I. Elsherif, S. El-Wakeel, Factors influencing lead and iron release from some Egyptian drinking water pipes, J. Hazard. Mater., 160 (2008) 675–680.
[7] USEPA, Office of Water Health and Ecological Criteria Division, Drinking Water Health Advisory for Manganese, Washington, D.C., 2004.
[8] WHO, Guidelines for Drinking-water Quality, 3rd ed., World Health Organization, Geneva, Vol. 1, 2008, p. 973.
[9] The Council of the European Union, The Quality of Water Intended for Human Consumption, Directive 98/83/EC, 1998.
[10] N. Kothari, Groundwater, iron and manganese: an unwelcome trio, Water Eng. Manage., 135 (1988) 25–26.
[11] D. Barloková, J. Ilavský, Removal of iron and manganese from water using filtration by natural materials, Polish J. Environ. Stud., 19 (2010) 1117–1122.
[12] S.C. Homoncik, A.M. MacDonald, K.V. Heal, B.É.Ó. Dochartaigh, B.T. Ngwenya, Manganese concentrations in Scottish groundwater, Sci. Total Environ., 408 (2010) 2467–2473.
[13] D.L. Varner, S. Skipton, D. Hay, P.J. Jasa, G96-1280 Drinking Water: Iron and Manganese, DigitalCommons@University of Nebraska - Lincoln, 1996.
[14] A. Takeda, Manganese action in brain function, Brain Res. Rev., 41 (2003) 79–87.
[15] R. Kawamura, H. Ikuta, S. Fukuzumi, R. Yamada, S. Tsubaki, T. Kodama, S. Kurata, Intoxication by manganese in well water, Kitasato Arch. Exp. Med., 18 (1941) 145–169.
[16] A. Woolf, R. Wright, C. Amarasiriwardena, D. Bellinger, A child with chronic manganese exposure from drinking water, Environ. Health Perspect., 110 (2002) 613–616.
[17] W.R. Knocke, S.C. Occiano, R. Hungate, Removal of soluble manganese by oxide-coated filter media: sorption rate and removal mechanism issues, J. Am. Water Works Assoc., 83 (1991) 64–69.
[18] S. Babel, T.A. Kurniawan, Low-cost adsorbents for heavy metals uptake from contaminated water: a review, J. Hazard. Mater., 97 (2003) 219–243.
[19] D. Barlokova, Natural zeolites in the water treatment process, Slovak J. Civ. Eng., 16 (2008) 8–12.
[20] L.V. Serikov, E.A. Tropina, L.N. Shiyan, F.H. Frimmel, G. Metreveli, M. Delay, Iron oxidation in different types of groundwater of Western Siberia, J. Soils Sediments, 9 (2009) 103–110.
[21] L. Serikov, L.N. Shiyan, E. Tropina, Oxidation of Different Forms of Iron Compositions in the Underground Water, Science and Technology, KORUS 2004, Proc. 8th Russian-Korean International Symposium, IEEE, 2004, pp. 82–84.
[22] N. Yavorovsky, S. Peltsman, J. Komev, Y.V. Volkov, Technology of Water Treatment using Pulsed Electric Discharges, Science and Technology, KORUS 2000, Proc. 4th Korea-Russia International Symposium, IEEE, 2000, pp. 422–427.
[23] M.A. Malik, A. Ghaffar, S.A. Malik, Water purification by electrical discharges, Plasma Sources Sci. Technol., 10 (2001) 82.
[24] E. Okoniewska, J. Lach, M. Kacprzak, E. Neczaj, The removal of manganese, iron and ammonium nitrogen on impregnated activated carbon, Desalination, 206 (2007) 251–258.
[25] P. Mondal, C. Majumder, B. Mohanty, Effects of adsorbent dose, its particle size and initial arsenic concentration on the removal of arsenic, iron and manganese from simulated ground water by Fe^{3+} impregnated activated carbon, J. Hazard. Mater., 150 (2008) 695–702.
[26] S. Xia, J. Nan, R. Liu, G. Li, Study of drinking water treatment by ultrafiltration of surface water and its application to China, Desalination, 170 (2004) 41–47.
[27] R. Hedges, M. McLellan, On the cation exchange capacity of fired clays and its effect on the chemical and radiometric analysis of pottery, Archaeometry, 18 (1976) 203–207.

[28] C. Giles, T. MacEwan, S. Nakhwa, D. Smith, 786. Studies in adsorption. Part XI. A system of classification of solution adsorption isotherms, and its use in diagnosis of adsorption mechanisms and in measurement of specific surface areas of solids, J. Chem. Soc. (1960) 3973–3993.
[29] APHA, Standard Methods for the Examination of Water and Wastewater, 21st ed., APHA, AWWA and WEF, Washington, D.C., 2005.
[30] B. Volesky, Biosorption process simulation tools, Hydrometallurgy, 71 (2003) 179–190.
[31] T. Bohli, I. Villaescusa, A. Ouederni, Comparative study of bivalent cationic metals adsorption Pb(II), Cd(II), Ni(II) and Cu(II) on olive stones chemically activated carbon, J. Chem. Eng. Process Technol., 4 (2013).
[32] W. Cai, G. Duan, Y. Li, Hierarchical Micro/Nanostructured Materials: Fabrication, Properties, and Applications, CRC Press, 2014.
[33] I. Langmuir, The adsorption of gases on plane surfaces of glass, mica and platinum, J. Am. Chem. Soc., 40 (1918) 1361–1403.
[34] M.M. Dubinin, E. Zaverina, L. Radushkevich, Sorption and structure of active carbons. I. Adsorption of organic vapors, Zhurnal Fizicheskoi Khimii, 21 (1947) 1351–1362.
[35] Y. Ho, C. Huang, H. Huang, Equilibrium sorption isotherm for metal ions on tree fern, Process Biochem., 37 (2002) 1421–1430.
[36] B. Volesky, Equilibrium Biosorption Performance, Sorption and Biosorption. CRC Press, Boca Raton, FL, USA, 2004, pp. 106–116.
[37] F.A. Al-Rub, M. El-Naas, F. Benyahia, I. Ashour, Biosorption of nickel on blank alginate beads, free and immobilized algal cells, Process Biochem., 39 (2004) 1767–1773.
[38] F.G. Helfferich, Ion Exchange, Courier Corporation, 1962.
[39] W. Rieman, H.F. Walton, Ion Exchange in Analytical Chemistry: International Series of Monographs in Analytical Chemistry, Elsevier, 2013.
[40] H.S. Ibrahim, N.S. Ammar, H.H. Abdel Ghafar, M. Farahat, Adsorption of Cd(II), Cu(II) and Pb(II) using recycled waste glass: equilibrium and kinetic studies, Desal. Wat. Treat., 48 (2012) 320–328.